

# Performance Analysis of IEEE 802.11ax OFDMA-based Multi-Channel Random Access

Yang Hang, Der-Jiunn Deng, *Member, IEEE*, and Kwang-Cheng Chen, *Fellow, IEEE*

**Abstract**—With the progressive increase of dense WiFi networks deployment, quality-of-experience (QoE) and power saving have become critical issues. IEEE 802.11ax, the task group aimed at High Efficient WLAN (HEW), is to handle this dense scenario. 802.11ax makes revolutionary modifications on both MAC and PHY layer. Especially one feature on MAC layer is OFDMA-based Multi-Channel Random Access (MCRA) mechanism. Using a 2-dimensional Markov chain model, we develop a framework to analyze the performance of the OFDMA-based MCRA and derive a closed-form expression of system efficiency and access delay. Our simulation results validate the accuracy of the theoretical analysis. Finally, the effects of system parameters, including the number of resource units (RUs) for random access, initial and maximum contention window, are estimated.

**Index Terms**—MCRA, Multi-User PHY, OFDMA, 802.11ax

## I. INTRODUCTION

During last decade, IEEE 802.11 has achieved a great success with enormous WiFi networks deployed for its high throughput and relative simplicity of implementation. According to Cisco Visual Network index [1], the mobile traffic will increase 53% at CAGR within 2015- 2020, i.e., eightfold, reaching 30.6 EB per month by 2020. Therefore, scenarios of WiFi networks will become the *dense scenarios*, which means plenty of stations (STA) or access points (AP) or both exist in a limited area. In this paper, the case of single AP with multiple STAs is our concern.

Actually, a series of standards (802.11b/g/n/ac) have evolved to handle the increasing WLAN demand. The method is mainly by means of raising data rate on the physical layer (PHY) from 2 Mbps to 7 Gbps [2]. However, performance or user experience of WiFi networks does not improve enough with the data rate, especially in the dense scenario. That is because the bottleneck of dense WiFi networks gradually relocates at MAC layer. The MAC is always based on distributed coordination function (DCF) in legacy 802.11, which is protocol on a Single-User (SU) PHY. Previous 802.11 amendments made fewer changes on MAC layer compared with that of PHY layer. And collisions consume many spectrum resource in the dense scenario.

MAC efficiency is mainly wasted by two causes, the overhead of control signaling and packet collisions. Much effort has been conducted in legacy 802.11 to reduce the overhead of control signaling, such as Reduced Inter-Frame Spacing

(RIFS), frame aggregation, etc [2]. In the dense scenario, collisions will be the major component of spectrum waste. That is why bottleneck relocates at MAC layer. The collision is caused by two problems, problem of unstable DCF and unfair queueing problem.

First, DCF is inherently unstable as it is a random access protocol. Collisions will consume even more spectrum resource in the dense scenario. Secondly, as we can see the WiFi network with queueing model, WiFi network will be an unfair queue, which will worsen the effect of the instability of DCF. Here we assume each STA and AP are modeled as an individual queue, and the shared channel is seen as the server. The WiFi network operates in a star topology, AP as the coordinator and  $n$  STAs nearby. On one hand, each STA and AP have the same chance to access the channel. On the other hand, all STAs obtain data from AP, which is referred to as down-link (DL) traffic, and the traffic from STAs to AP as up-link (UL) traffic. Thus the AP shares the DL traffic loading, which accounts for more than  $1/2$  of total traffic, while it only has  $1/(n+1)$  chance to access channel. The queue model of WiFi network is, therefore, an unfair queue between DL and UL transmissions.

Study group 802.11ax, aimed at HEW in the dense scenarios, thus modifies the MAC thoroughly by substituting DCF with centralized control. On the PHY layer, OFDMA is proposed to implement both the DL and UL Multi-User (MU) channel, which means a STA could communicate with multiple STAs simultaneously. On MAC layer, a brand new control frame called trigger frame (TF) is created to implement TF-based UL transmission. Thus the AP could schedule both DL and UL transmissions, which means DCF will be replaced by a scheduled MAC protocol. And instability of DCF will be mitigated very well and the unfair queueing problem will not exist anymore as AP does not need to contend with STAs. Moreover, an OFDMA-based multi-channel random access (MCRA) is proposed in 802.11ax as random access is highly efficient to transmit short frames, like bandwidth request. In the three-way handshake mechanism, AP initiates the MCRA by transmitting a TF at first. STAs receiving the TF then contends with Aloha and binary exponential backoff mechanism. AP finally responds with ACK telling which STAs succeed in contending. A random access procedure is thus composed of a three-way handshake. Details of the mechanism will be illustrated in Section II.

As for the OFDMA-based MCRA, we are concerned about number of stations succeeding in accessing the channel and access delay. Actually, while MCRA has been supported by cellular networks to perform initial association to the network

Jet Yu are Jordan Lee were with National Taiwan University.

Shao-Yu Lien is with Department of Electronic Engineering, National Formosa University, see (<http://sparc.nfu.edu.tw/sylien/>)

Fernando Rosas was with Department of Electrical Engineering, Pontificia Universidad Catolica de Chile, Santiago, Chile

and to request transmission resource, this is the first time for 802.11 to apply OFDMA shifting SU PHY to MU PHY. In recent years, related works have proposed some models to derive the throughput [3] [4] [5], the collision probability [6] [7], and the access delay [3] [6] [7] [8]. [3] gives a closed-form expression of throughput for OFDMA system. [4] proposes a stabilized multi-channel slotted Aloha algorithm. And [5] designs a 1-persistent type retransmission that avoids exponential backoff to achieve a fast access. Some other works [3] [7] [6] compare performance of two kinds of backoff mechanism, binary exponential backoff and uniform backoff, which are implemented by IEEE 802.16 and 3GPP LTE respectively. [9] specifies a model estimating transient behavior of OFDMA system. In addition, unlike [11], [10] generalizes CSMA/CA to OFDMA system for 802.11.

In this paper, the steady state behavior of the OFDMA-based MCRA is evaluated by extending Bianchi's Markov chain model [12], which has never been used to model the OFDMA-based MCRA before. Though the MCRA differs much from DCF, including SU channel to MU channel, distributed MAC scheme to centralized MAC scheme and carrier sense to Aloha, Bianchi's Markov chain model is validated in this paper that it could be extended to precisely model the MCRA mechanism. Thereby, we evaluate the system efficiency, access delay and effects of important system parameters.

The paper is organized as follows. We firstly explain features of 802.11ax features including OFDMA MU and OFDMA-based random access procedure in Section II. Section III contains the system model. Then Section IV shows simulation results, along with analysis results to validate the model. Additional considerations on optimal performance are carried out in Section V-A. After that, Section V evaluates the effects of some important system parameters. Conclusion remark is finally given in Section VI.

## II. 802.11AX FEATURES

Necessary features of 802.11ax to understand the OFDMA-based MCRA mechanism are illustrated in this section. As stated above, collisions in dense scenario degrade the performance of WiFi networks as the bottleneck locates at MAC. Study group 802.11ax thus proposes TF-based UL procedure, which means UL transmission could be scheduled by AP, shifting distributed MAC to centralized MAC. on the other hand, OFDMA is issued in IEEE 802.11ax to realize MU PHY. And OFDMA-based multi-channel random access (MCRA) is proposed. For more features of 802.11ax, [13] is a good reference.

### A. MU PHY

Though MU PHY has been implemented in 802.11n and 802.11ac with MU-MIMO, which only realizes MU DL transmission, OFDMA is adopted by 802.11ax to implement both MU DL and MU UL transmissions. Especially for MU UL transmission, which is more difficult to implement compared with MU DL transmission, trigger-based MU UL is proposed.

With MU PHY, the original SU 20 MHz channel could be specified more fine-grained and be also aggregated to a wider

TABLE I: Maximum number of RUs for each channel width

RU type	CBW20	CBW40	CBW80	CBW80+80 and CBW160
26-tone RU	9	18	37	74
52-tone RU	4	8	16	32
106-tone RU	2	4	8	16
242-tone RU	1	2	4	8
484-tone RU	N/A	1	2	4
996-tone RU	N/A	N/A	1	2
2×996 tone RU	N/A	N/A	N/A	1

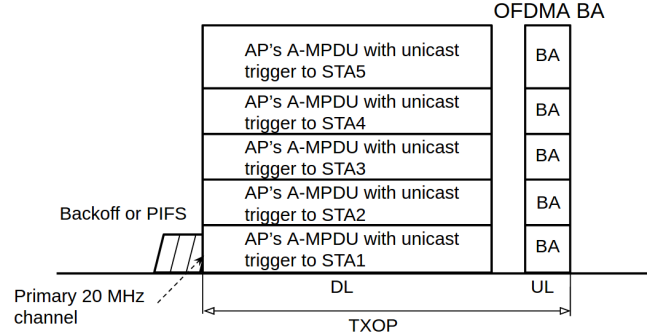


Fig. 1: MU DL of 802.11ax

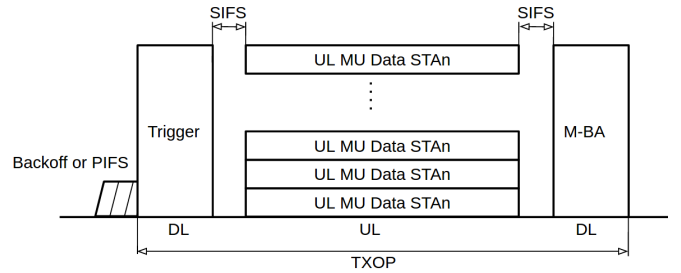


Fig. 2: Trigger-based MU UL of 802.11ax

channel to meet various bandwidth demands. The resource unit (RU), which can be accessed by one STA, is specified as Table I. For example, the smallest RU is 26-tone, with which a 20 MHz could be separated into 9 subchannels. Also multiple 20 MHz channels can be aggregated to improve system throughput, which is referred to as *Channel Bonding*. It is worth mentioning that every transmission of MU should end at the same time. That means padding is required for shorter packets.

In respect of MAC layer, first for MU DL transmission, AP transmits DL packets to multiple stations simultaneously as in Fig. 1. Secondly, MU UL transmission is a little complicated as WiFi network is not a well-synchronized system, where preamble and acknowledgement mechanisms are required for a data packet transmission. A trigger-based MU UL transmission is thus issued as in Fig. 2. A brand new control frame, trigger frame (TF), is created to be transmitted by AP to initiate the UL transmission. STAs could not transmit UL packets until they receive a TF which allocates RU for the STA or for random access. Afterwards, AP responds with ACK frame, forming a three-way handshake UL transmission. The trigger frame format is as in Fig. 3. Since the standard is in progress, some fields remain to be determined (TBD). In the field *User*

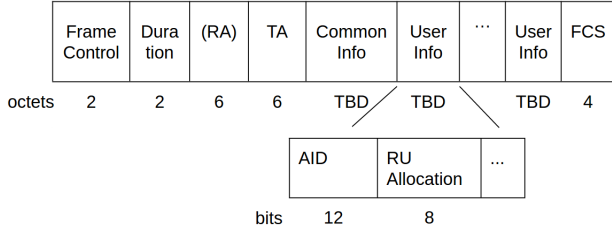


Fig. 3: Trigger Frame format

*Info*, subfield *AID* represents the identification of STA and subfield *RU Allocation* represents the RU allocated to the STA. Especially, *AID* with value 0 means the RU is for random access.

### B. OFDMA-based MCRA

An example of TF-based MU UL transmission with OFDMA-based MCRA, illustrated as in Fig. 4, is divided into two steps, one as random access procedure and the other UL data transmission. Random access procedure, namely the OFDMA-based MCRA, works as collecting traffic information from stations. Thereby in the next step, AP could allocate RUs to STAs by transmitting a TF containing RU allocation. Then the STAs, receiving the TF with resource allocation information, transmit UL data packets. And AP at last responds ACK. Therefore, TF above in the example have two variants, one for random access and the other for resource allocation. The key of this mechanism locates at random access, i.e., the OFDMA-based MCRA, which is our concern.

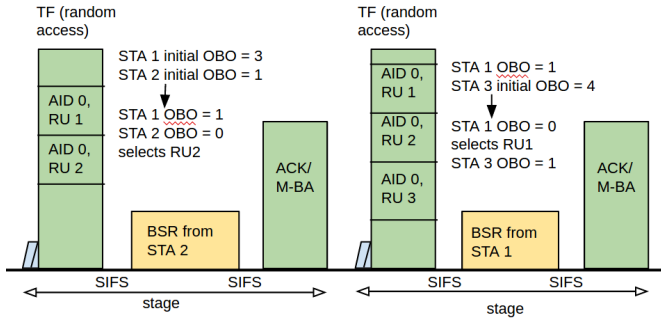


Fig. 5: Illustration of OFDMA-based MCRA

Details of OFDMA-based MCRA mechanism is as Fig. 5. To initialize a random access procedure, AP first transmits a TF announcing RUs for random access by setting the AID of the RUs to 0. Attempting STAs, whose buffers are not empty, maintain a backoff counter named OFDMA Backoff (OBO), which are randomly generated among range  $[0, OCW]$ . Then the OBO subtracts the value of  $M$  once receiving the TF, otherwise freezes, where  $M$  is calculated by sum the number of RUs whose AID equals 0. When the OBO reaches 0, the STA will randomly select a RU from those whose AIDs equal 0 to transmit a request after short inter-frame spacing (SIFS). After that, AP responds with a block-ACK indicating which STAs contend successfully. The period of the whole three-way handshaking is named a *stage*. A successful stage means

at least one STA contend successfully to transmit a request in a stage. It is worth noting that the stage in this paper, which is specified from standard [11], is a concept of the time interval, not the backoff stage in other papers. To avoid confusion of the two meanings, backoff stage is replaced with *backoff level* in this paper. When STAs fail to contend, the *OCW* will be doubled until *OCW* reaches  $OCW_{max}$ , which means the backoff level increases one step once a failure until the highest level.

In terms of implementation, system parameters of the MCRA are configured dynamically by AP, including  $OCW_{min}$ ,  $OCW_{max}$ ,  $M$ , where  $OCW_{min}$ ,  $OCW_{max}$  represent the minimum and the maximum contention window, and  $M$  as the number of RUs for random access. Two of critical parameters  $OCW_{min}$ ,  $OCW_{max}$  are configured in Random Access Parameter Set (RAPS) element contained in beacon frame sent by AP. Check field *OCW Range* in RAPS element as in Fig. 6,  $OCW_{min} = 2^{EOCW_{min}} - 1$ ,  $OCW_{max} = 2^{EOCW_{max}} - 1$ .  $M$  is obtained from TF by sum the number of RUs whose AID equal 0. To simplify following analysis, we issue another parameter  $m$ , *maximum backoff level*, so that  $OCW_{max} = (OCW_{min} + 1) * 2^m - 1$ . The configuration of system parameter is absolutely different from that of legacy 802.11, where all the parameters are predefined in each STA's hardware. OFDMA-based MCRA is thus more flexible compared with DCF.

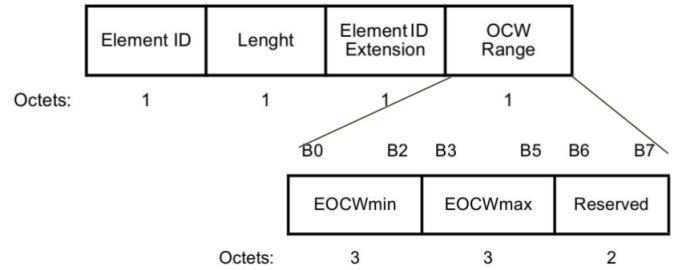


Fig. 6: Random Access Parameter Set (RAPS) Element

## III. SYSTEM MODEL

Bianchi's Markov chain model has been validated that it accurately depicts the steady state behavior of DCF based on the assumption that at each request transmission, and regardless of the number of retransmission suffered, each request frame collides with constant and independent probability  $p$ . Although some differences exist between OFDMA-based MCRA and DCF, we have validated that OFDMA-based MCRA could be modeled with Markov chain model.

The analysis is divided into two parts. First is the Markov chain model to estimate the packet transmission probability  $\tau$  and conditional collision probability  $p$ . Secondly, we evaluate some metrics given  $\tau$ , including the number of stations who succeed in contending in a stage  $n_s$ , self-defined system efficiency  $eff$ , and expected access delay of a STA  $D$ . Table II is a list of all parameters and notations.

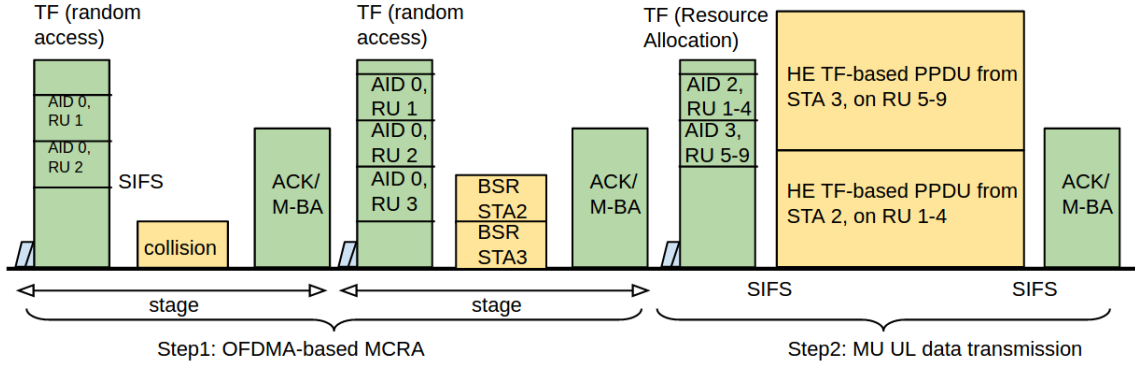


Fig. 4: An example of Trigger-based MU UL transmission with OFDA-based MCRA

TABLE II: Parameters and Notations Interpretation

Notations	Meaning
$n$	Number of stations
$OCW_{min} (W_0)$	Minimum OFDMA contention window
$OCW_{max} (W_m)$	Maximum OFDMA contention window
$M$	Number of RUs for random access
$m$	Maximum backoff level
$p$	Packet collision probability
$\tau$	Station's transmission probability
$n_s$	Number of successful stations in a stage
$D$	Access delay, number of stages for a station to contend successfully

#### A. Packet Transmission Probability

Consider a fixed number  $n$  of stations under saturation condition, which means each station is an attempting station. For saturation analysis, stage of MCRA is one after another. Also, the ideal channel is assumed so that collision happens only if more than one station transmits at the same RU. Since the critical of the mechanism is OFDMA-based MCRA, only UL request transmission is concerned, while DL transmission and UL data transmission are not considered here.

To model OFDMA-based MCRA with the discrete-time Markov chain model, the concept of time is supposed to be adapted. In DCF, time unit of the model corresponds with slot, while in OFDMA-based MCRA time unit of the model is stage, a three-way handshake. Thus the delay will be measured in the number of stages.

Similar to Bianchi's work, let  $\{s(t), b(t)\}$  be the bi-dimension process, where  $s(t)$  denotes the backoff level  $(0, \dots, m)$ , and  $b(t)$  denotes backoff counter  $(0, \dots, W_i)$ . With the discrete and integer time scale,  $t$  and  $t+1$  corresponds to beginnings of two consecutive stages.  $\{b(t)\}$  is not Markov process because the state of the current stage depends on the history of transmission instead of only the previous stage. The bi-dimensional process  $\{s(t), b(t)\}$  is also a Markov chain. The key assumption is still necessary that at each request transmission, and regardless of the number of retransmission suffered, each request frame collides with constant and independent probability  $p$ . With the independence assumption,  $p$  will be a constant. The Markov chain is able to be conducted as in Fig. 7.

Another important difference between the two Markov chain models of OFDMA-based MCRA and DCF, is clarified here.

Since the station of DCF senses the carrier before transmitting, it will freeze its backoff counter and stay at the state if channel is sensed busy. However in the OFDMA-based MCRA, because the time unit, a stage, contains a period for exactly a packet transmission, stations certainly subtract  $M$  from the OBO only if they receive a TF for random access. Stations of the MCRA thus stay in one state for a period of exactly single stage.

Some modifications are mentioned here to adapt to differences between OFDMA-based MCRA and DCF. First, in a row of states, as OBO subtracts the value of  $M$  rather than 1, stations transfer to states  $M$ -step ahead. Second, since states with  $b(t) \leq M$  will decrease to 0 at the current state, which means stations could access RUs, we could merge these states into one state, denoted by  $\{i, T\}$ .  $T$  is an integer set of  $[0, M]$ .

Let's assume  $P\{i_1, k_1 | i_0, k_0\} = P\{s(t+1) = i_1, b(t+1) = k_1 | s(t) = i_0, b(t) = k_0\}$ . In this Markov Chain, the only non null one-step transition probabilities are

$$\begin{cases}
 P\{i, T | i, k\} = 1 & k \in [M+1, 2M] \quad i \in [0, m] \\
 P\{i, k-M | i, k\} = 1 & k \in [2M+1, W_i] \quad i \in [0, m] \\
 P\{0, k | i, T\} = \frac{1-p}{W_0+1} & k \in [M+1, W_0] \quad i \in [0, m] \\
 P\{0, T | i, T\} = \frac{(1-p)(M+1)}{W_0+1} & i \in [0, m] \\
 P\{i, k | i-1, T\} = \frac{p}{W_i+1} & k \in [M+1, W_i] \quad i \in [1, m] \\
 P\{i, T | i-1, T\} = \frac{p(M+1)}{W_i+1} & i \in [1, m] \\
 P\{m, k | m, T\} = \frac{p}{W_m+1} & k \in [M+1, W_m] \\
 P\{m, T | m, T\} = \frac{p(M+1)}{W_m+1}
 \end{cases} \quad (1)$$

The first and second equations in (1) accounts for the fact that the backoff counter maintained by stations will subtract  $M$ , the number of RUs for random access. The third and fourth equations represent that after a successful contention, stations will reset the contention window size to initial window size and uniformly generate a backoff value among  $[0, W_0]$ , since  $T$  is an integer set  $[0, M]$ , the transition probability to states  $\{i, T\}$  is  $M+1$  times of that to states  $\{i, k\}$ . For the fifth and sixth equations, they represent when a failure contention occurs, the contention window size will be doubled,  $W_i = 2W_{i-1} + 1$ . The last two equations are the case of failure at the maximum backoff level. We assume no packets are discarded, repeating retransmitting until success.

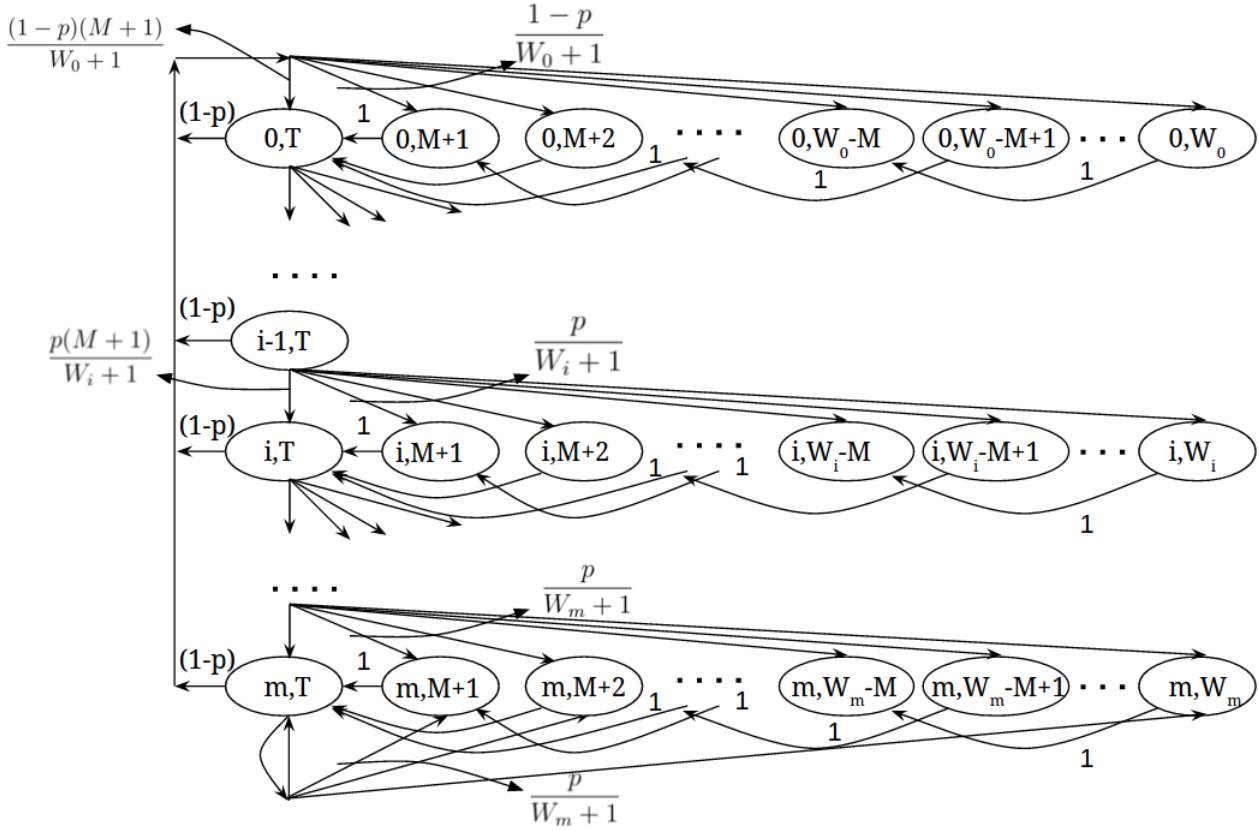


Fig. 7: Markov Chain model for the backoff window size

Let  $b_{i,k} = \lim_{t \rightarrow \infty} P\{s(t) = i, b(t) = k\}$ ,  $i \in [0, m]$ ,  $k \in [0, W_i]$ , be the stationary distribution of the Markov chain. Then we show how to obtain transmission probability  $\tau$  and conditional collision probability  $p$ . First, for states with  $b(t) = T$ , in which stations will transmit requests or BSRs in current stage,

$$\begin{aligned} b_{i-1,T} \cdot p &= b_{i,T} \rightarrow b_{i,T} = p^i b_{0,T}, \quad 0 \leq i < m \\ b_{m-1,T} \cdot p &= (1-p)b_{m,T} \rightarrow b_{m,T} = \frac{p^m}{1-p} b_{0,T}. \end{aligned} \quad (2)$$

Then, other states are expressed with states in which  $b(t) = T$ :

$$b_{i,k} = \begin{cases} (\lfloor \frac{W_0-k}{M} \rfloor + 1) \frac{(1-p)}{W_0+1} \sum_{i=0}^m b_{i,T}, & M+1 \leq k \leq W_0, \quad i=0 \\ (\lfloor \frac{W_i-k}{M} \rfloor + 1) \frac{p}{W_i+1} b_{i-1,T}, & M+1 \leq k \leq W_i, \quad 0 < i < m \\ (\lfloor \frac{W_m-k}{M} \rfloor + 1) \frac{p}{W_m+1} (b_{m-1,T} + b_{m,T}), & M+1 \leq k \leq W_m, \quad i=m \end{cases} \quad (3)$$

From (2),  $\sum_{i=0}^m b_{i,T} = \frac{b_{0,T}}{1-p}$  is obtained; whereby (3) could be summed respectively to get (4).

Each subequation in (4) has the same term:  $-\frac{M}{2} \lfloor \frac{W_i}{M} \rfloor^2 + (W_i - \frac{M}{2}) \lfloor \frac{W_i}{M} \rfloor$ . To simplify the expression, let  $X_i = -\frac{M}{2} \lfloor \frac{W_i}{M} \rfloor^2 + (W_i - \frac{M}{2}) \lfloor \frac{W_i}{M} \rfloor$ . Then, sum the steady state probability of all states to get (6).

whereby a closed-form expression of  $\tau$ , the probability of a station transmitting a request at a stage, is derived.

$$\tau = \sum_{i=0}^m b_{i,T} = \frac{b_{0,T}}{1-p} = \frac{W_0+1}{W_0+1 + (1-p)X_0 + (1-p) \sum_{i=1}^{m-1} X_i \left(\frac{p}{2}\right)^i + X_m \left(\frac{p}{2}\right)^m} \quad (7)$$

For  $m = 0, M = 1$  which is SU PHY with a fixed contention window, check (5), the terms containing  $X_i, i > 0$  will disappear, and  $b_{0,T}/(1-p)$  degrades to  $b_{0,T}$ . As a result, (6) degrades to

$$1 = b_{0,T} \left( \frac{W_0+1+X_0}{W_0+1} \right). \quad (8)$$

Thereby,

$$\begin{aligned} \tau &= b_{0,T} = \frac{W_0+1}{W_0+1+X_0} \\ &= \frac{2(W_0+1)}{W_0^2+W_0+2}, \end{aligned} \quad (9)$$

which is different from that of CSMA/CA with constant window size [14], where  $\tau = \frac{2}{W_0+1}$ . That is because stations of CSMA/CA freezes backoff counter when sensing busy channel while no such freeze mechanism of backoff counter exists in OFDMA-based MCRA.



$$\begin{cases} \sum_{k=M+1}^{W_0} b_{0,k} = \frac{b_{0,T}}{W_0+1} \left( -\frac{M}{2} \left\lfloor \frac{W_0}{M} \right\rfloor^2 + (W_0 - \frac{M}{2}) \left\lfloor \frac{W_0}{M} \right\rfloor \right) \\ \sum_{i=1}^{m-1} \sum_{k=M+1}^{W_i} b_{i,k} = \frac{b_{0,T}}{W_0+1} \left( \frac{p}{2} \right)^i \left( -\frac{M}{2} \left\lfloor \frac{W_i}{M} \right\rfloor^2 + (W_i - \frac{M}{2}) \left\lfloor \frac{W_i}{M} \right\rfloor \right) \\ \sum_{k=M+1}^{W_m} b_{m,k} = \frac{b_{0,T}}{W_0+1} \frac{(\frac{p}{2})^m}{1-p} \left( -\frac{M}{2} \left\lfloor \frac{W_m}{M} \right\rfloor^2 + (W_m - \frac{M}{2}) \left\lfloor \frac{W_m}{M} \right\rfloor \right) \end{cases} \quad (4)$$

$$1 = \sum_{i=0}^m \sum_{k=0}^{W_i} b_{i,k} = \frac{b_{0,T}}{W_0+1} \left( X_0 + \sum_{i=1}^{m-1} X_i \left( \frac{p}{2} \right)^i + X_m \frac{(\frac{p}{2})^m}{1-p} \right) + \frac{b_{0,T}}{1-p} \quad (5)$$

$$= b_{0,T} \left( \frac{(1-p)X_0 + (1-p) \sum_{i=1}^{m-1} X_i \left( \frac{p}{2} \right)^i + X_m \left( \frac{p}{2} \right)^m + W_0 + 1}{(W_0+1)(1-p)} \right), \quad (6)$$

On the other hand, conditional collision probability  $p$  has another relation with the probability  $\tau$ . With ideal channel assumption that the collision happens only if at least one of other stations select the same RU, we have

$$p = 1 - \left( 1 - \frac{\tau}{M} \right)^{n-1}. \quad (10)$$

Rewrite (10) as  $\tau^* = \left( 1 - (1-p)^{\frac{1}{n-1}} \right) M$ . To obtain probability  $\tau$  and  $p$ , we need to find solutions to a group of the two equations 7 and 10.  $\tau^*(p)$  is a monotonically increasing function. Though  $\tau(p)$  is hard to determine the monotonicity from the expression of equation 7 with respect to  $p$ , the function 7 is estimated monotonically decreasing by numerical method. Also,  $\tau(0) = \frac{W_0+1}{W_0+1+X_0} > \tau^*(0) = 0$ . And  $\tau(1) < \tau^*(1) = M$ . Therefore, the only solution could be found by numerical method.

### B. Random Access Efficiency

With the transmission probability  $\tau$ , performance of OFDMA-based MCRA mechanism could be easily evaluated. First, the expected number of stations who contend successfully at a stage, denoted by  $E[n_s]$ . Extending  $n_s$ , a system efficiency is defined as another important metric. Also, the access delay denoted by  $D$ , referred to as number of stages required for a station to contend successfully, could be derived.

1)  $n_s$  and System Efficiency: What we are concerned about is that how many stations contend successfully at a stage. Given  $\tau$  and  $p$ , the probability that a station contend successfully in a stage is firstly derived:  $P_{s\_station} = \tau(1-p)$ . Then, with (10),  $E[n_s]$  is easily expressed as follows.

$$\begin{aligned} E[n_s] &= n P_{s\_station} \\ &= n \tau (1-p) \\ &= n \tau \left( 1 - \frac{\tau}{M} \right)^{n-1} \end{aligned} \quad (11)$$

Furthermore, normalizing  $n_s$ , system efficiency here is defined as the ratio of the number of successful contending

stations in a stage to the number of RUs for random access in a stage.

$$\begin{aligned} \text{eff}(\tau) &= \frac{E[n_s]}{M} \\ &= \frac{n \tau \left( 1 - \frac{\tau}{M} \right)^{n-1}}{M} \end{aligned} \quad (12)$$

2) Access Delay:  $D$  represents the number of stages required for a station to contend successfully in a stage. Because of saturation assumption, a new request arrives once one previous request is transmitted successfully. Thus queueing waiting time is not considered here. In this way, the access delay  $D$  follows the geometric distribution with parameter  $P_{s\_station}$ , which is obtained just now. Then the expected value of access delay of request frame,  $E[D]$ , is

$$E[D] = \frac{1}{\tau \left( 1 - \frac{\tau}{M} \right)^{n-1}}. \quad (13)$$

## IV. MODEL VALIDATION

The same with scenario for analysis, only OFDMA-based MCRA mechanism, i.e., Fig. 5, is concerned. Simulation runs with three-way handshake stage by stage. We run simulations for 1,000,000 stages with a variety of parameter sets  $\{M, OCW_{min}, OCW_{max}\}$  and collects the information of the two variables, the number of successful attempt STAs  $n_s$  and expected access delay  $D$ . The values of results from both analysis and simulation are given in Fig. 8 and Table III. The results show that the Markov model precisely predicts the steady state behavior of the OFDMA-based MCRA mechanism.

## V. PERFORMANCE EVALUATION

With above analysis, we could conveniently evaluate performance, including system efficiency and access delay, and the effects of system parameters. Since the model acts quite precisely, model analysis is solicited to evaluate the performance later.

TABLE III: Analysis versus simulation:  $n_s$  and access delay with  $m = 3, M = 9, OCW_{min} = 15$

$n_s$	analysis	simulation
$n = 1$	0.72727	0.72728
$n = 5$	2.23001	2.22335
$n = 10$	2.88954	2.88546
$n = 20$	3.29798	3.29857
delay	analysis	simulation
$n = 1$	1.37500	1.37499
$n = 5$	2.24214	2.24886
$n = 10$	3.46075	3.46565
$n = 20$	6.06432	6.06323

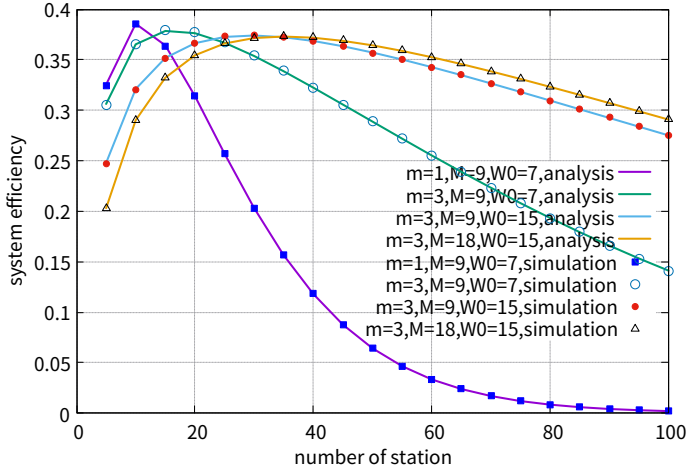


Fig. 8: System efficiency: Analysis versus Simulation

#### A. Maximum System Efficiency and Minimum Access Delay

With the system efficiency given in (12), take the derivative with respect to  $\tau$ , and find the extreme point,  $\tau^* = M/n$ . Since  $\tau \in [0, 1]$ ,  $\tau^* = \min\{1, M/n\}$ . In the dense scenario, i.e.,  $n$  is large, then  $\tau^* = M/n$ . The system efficiency thus is

$$\text{eff}(\tau^*) = (1 - \frac{1}{n})^{n-1} \quad (14)$$

Then the maximum  $n_s$  is

$$E[n_s]^* = M \cdot \text{eff}(\tau^*) = M(1 - \frac{1}{n})^{n-1}. \quad (15)$$

The limit of system efficiency, based on infinite  $n$ , is

$$\lim_{n \rightarrow \infty} \text{eff}(\tau^*) = \lim_{n \rightarrow \infty} (1 - \frac{1}{n})^{n-1} = \frac{1}{e} \quad (16)$$

which is the same with efficiency of SU slotted Aloha [15].

With the delay analysis given in (13), take the derivative with respect to  $\tau$ , and find the extreme point,  $\tau^* = M/n$ . Also,  $\tau^* = \min\{1, M/n\}$ . When  $n \geq M$ , the minimum access delay is

$$D(\tau^*) = \frac{n}{M(1 - \frac{1}{n})^{n-1}}. \quad (17)$$

From above analysis, we find that the maximum system efficiency and minimum access delay are both obtained by the  $\tau^* = \min\{1, M/n\}$ . What's more, optimal system efficiency is independent with  $M$ , while  $M$  affects access delay. The larger  $M$  is, the shorter the access delay will be. It indicates

that when AP allocates RUs for random access, the AP could allocate as many as possible.

Since  $\tau$  and  $p$  are obtained by solving group equations (7) and (10), it's hard to give a closed-form expression of  $\tau$  only depending on system parameters,  $M, W_0, m$  and  $n$ . The only way to catch the insights of the MCRA is to tune the system parameters  $\{M, W_0, W_m\}$  one by one.

#### B. RUs for Random Access $M$

(14) has indicated that  $M$ , has nothing to do with optimal system efficiency. However,  $n_s$  and  $D$  are proportional and inversely proportional to  $M$  respectively according to (15) and (17). Following analysis results validate the statement.

In Fig. 9a, the maximum system efficiency from various cases are almost the same, approaching  $1/e$ . The only difference is "where" the optimal point locates. Practically, the other two metrics,  $n_s$  and  $D$ , are closely related to  $M$ . Fig. 9b shows that larger  $M$  results more stations contend successfully in a stage. Moreover, Fig. 9c shows that larger  $M$  markedly decrease the access delay. Above all, when AP allocates RUs for random access, AP should allocate as many RUs as possible.

#### C. $OCW_{min}, OCW_{max}$

Fig. 10 shows case 1 ( $M = 9$ ) and case 2 ( $M = 18$ ), so that the rules we get are more convinced. In the figure, the purple line without point depicts the  $\tau^*$  that  $\tau^* = \min\{1, M/n\}$ . With above analysis and effects of  $M$ , we tune remaining parameters  $OCW_{min}, OCW_{max}$  so that  $\tau$  approaches the optimal line. To see the trend of the line clearly, larger  $n$  is configured so that some rules could be obtained as follows.

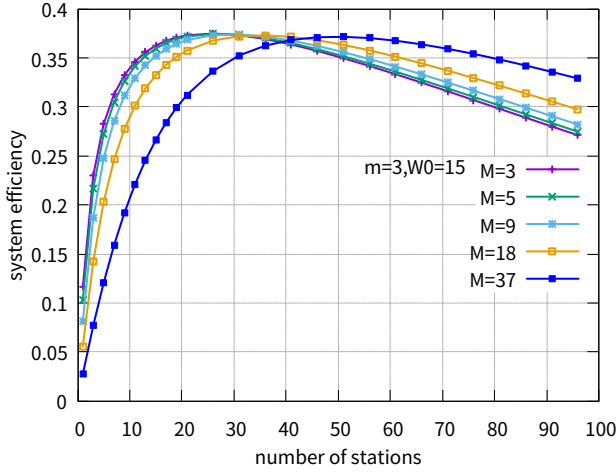
First, the  $OCW_{min}$  or  $W_0$ , determines  $\tau$  with small  $n$ . The larger  $W_0$  is, the lower  $\tau$  is at  $n = 1$ . That's why cases in Fig. 10 have two different start points.

Secondly,  $m = 0$  results in constant  $\tau$ , which is consistent with (9) that  $\tau$  does not depend on  $n$ . A special case,  $W_0 < M$  for scenario  $n \leq M$ , results in constant  $\tau$  equals to 1 regardless of  $n$ . It perfectly matches  $\tau^*$  at  $n \leq M$  as  $\tau^* = 1$  for the scenario  $n \leq M$ . Thus, if given  $n \leq M$ , the optimal configuration will be  $OCW_{max} = OCW_{min} < M$ .

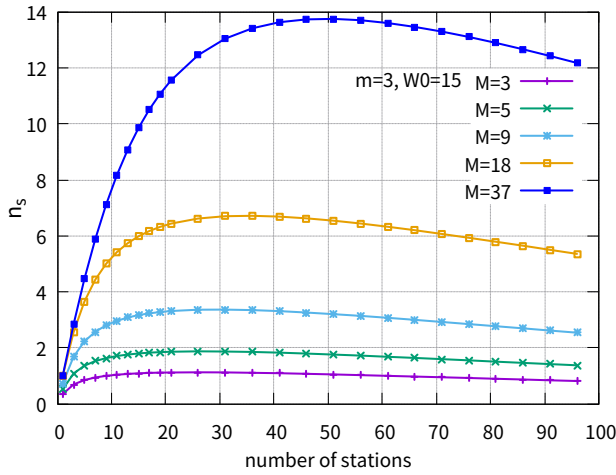
Thirdly, performance of the dense scenario strongly depends on  $OCW_{max}$ . It determines the limit of the  $\tau$ , i.e., where the line of  $\tau$  will converge. And both the two figures in Fig. 10 correspond with the above statement. And larger  $W_m$  causes lower  $\tau$ , which is closer to  $\tau^*$  when  $n$  is large.

Then, two subfigures as in Fig. 11 are generated from Fig. 10 with  $n$  ranges from  $[0, 100]$  to observe practical scenarios more clearly. Another observation whereby is that when  $W_0 = 1$ , line of  $\tau$  will have a flat start, which happens to match better with  $\tau^*$  at  $n \leq M$ .

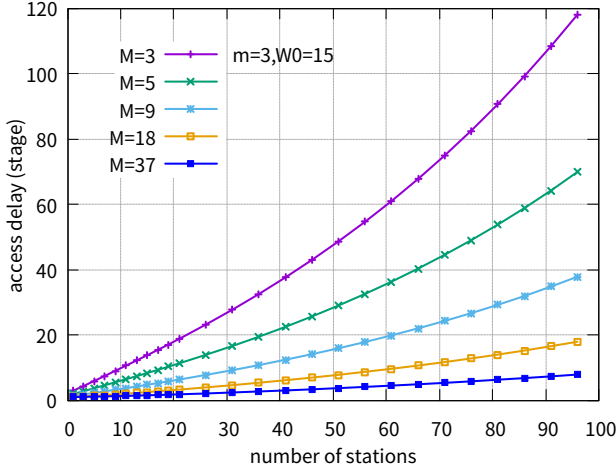
All above observations are summed up that  $W_0$  has significant influence on scenario of  $n \leq M$ , while  $W_m$  counts when  $n$  is large, namely the dense scenario. In the next two subsections, the system efficiency and access delay under different parameter configurations are practically evaluated, whereby above observed effects of parameters could be conformed.



(a) System efficiency versus number of stations



(b) Number of successful stations in a single stage versus number of stations



(c) Access delay versus number of stations

Fig. 9: Configure  $M$ 

1) *Configure  $OCW_{max}$* : With above rough rules, the effect of  $OCW_{max}$  is first evaluated by setting different  $OCW_{max}$  while fixing  $OCW_{min} = 1$  and  $M = 9$ . In Fig. 12a, three cases which has the same  $OCW_{min}$  are selected to clearly

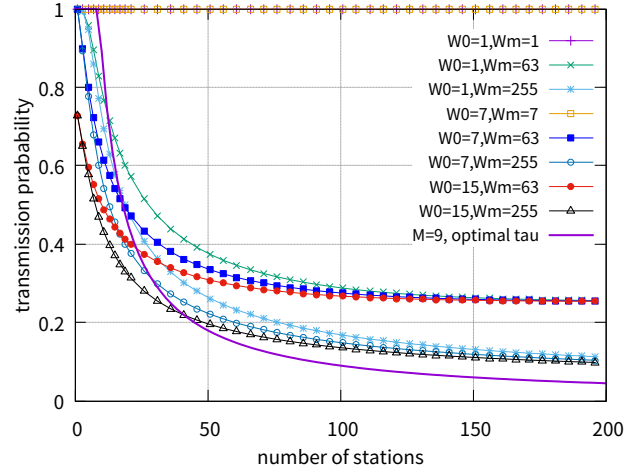
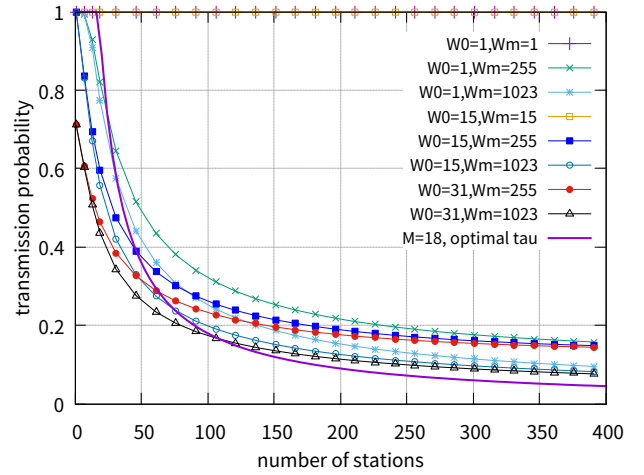
(a) Case 1, given  $M = 9$ (b) Case 2, given  $M = 18$ 

Fig. 10: Transmission probability versus number of stations

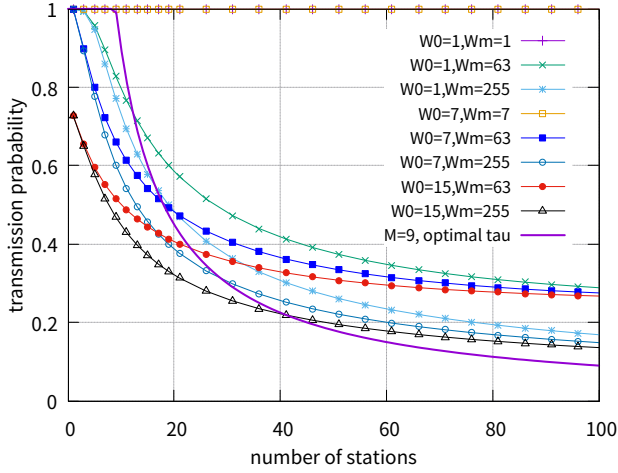
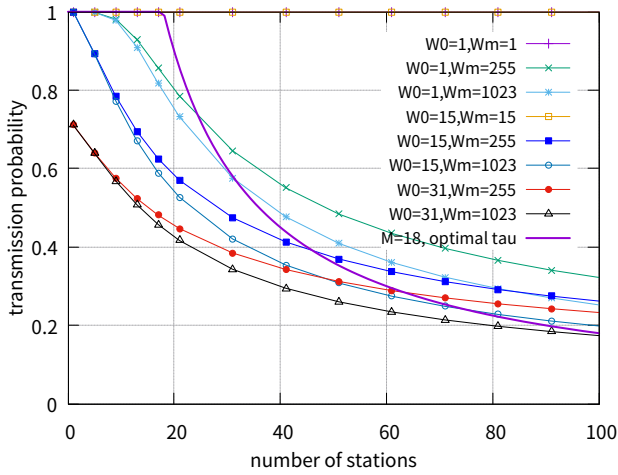
display the effect of  $OCW_{max}$  on system efficiency. From the figure, it is evident that larger  $OCW_{max}$  is much better for system efficiency when  $n \geq M$ . The result corresponds to the above rules obtained from the effect of parameters on  $\tau$ . Additionally, larger  $OCW_{max}$  results in shorter access delay.

2) *Configure  $OCW_{min}$* : To estimate the effect of  $OCW_{min}$ , the performance of different configurations of  $OCW_{min}$  while fixing large  $OCW_{max} = 1023$ , and  $M = 18$ . First,  $OCW_{min}$  determines the start of the probability  $\tau$ , and it has a significant influence on the scenario of  $n \leq M$ . From Fig. 13a and 13b, we find larger  $OCW_{min} = 127$  has lower system efficiency and larger access delay. Secondly, as stated in Section V-C that  $W_0 = W_m \leq M$  is the perfect configuration in the scenario of  $n \leq M$ , it is validated in Fig. 13 that maximum system efficiency and minimum access delay are achieved with the configuration in the scenario of  $n \leq M$ . However, the configuration of small  $OCW_{min}$  and large  $OCW_{max}$  almost achieves as good performance as the perfect configuration.

To this end, all observed rules are listed as follows.

- 1 For  $M$ : the larger the better



(a) Case 1, given  $M = 9$ (b) Case 2, given  $M = 18$ Fig. 11: Details of transmission probability versus number of stations when  $n \leq 100$ 

2 For  $OCW_{min}, OCW_{max}$ :

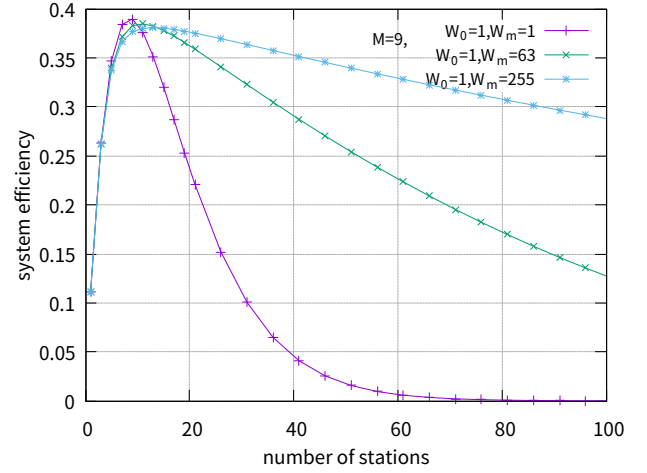
- $OCW_{min}$  counts when  $n \leq M$ . Smaller  $OCW_{min}$  is better.
- $OCW_{max}$  counts when  $n > M$ . Larger  $OCW_{max}$  is better.

• Special case: for  $n \leq M$

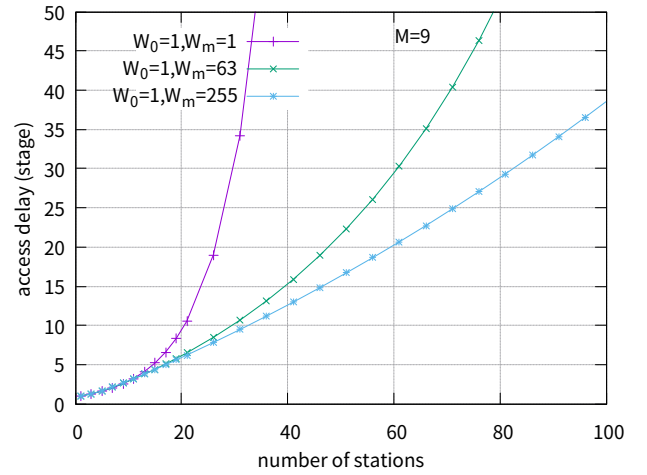
$OCW_{max} = OCW_{min} < M$  is the optimal configuration.

## VI. CONCLUSION

In this paper, Bianchi's Markov chain model is extended for saturation analysis of the OFDMA-based MCRA mechanism of 802.11ax. The simple Markov chain model is validated that it could precisely depict the steady state behavior of OFDMA-based MCRA of 802.11ax. Thereby, closed-form expressions of system efficiency and access delay are derived. Finally, it is observed that performance strongly depends on the system parameters. Larger number of RUs or subchannels for random access results in more successful contending stations at a stage. The initial contention window counts when only a



(a) System efficiency versus number of stations



(b) Access delay versus number of stations

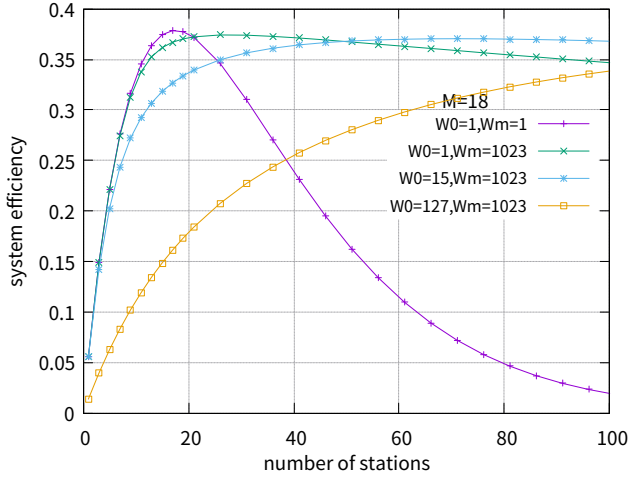
Fig. 12: Example of Configuring  $OCW_{max}$ , given  $M = 9$ 

few stations exist, while maximum contention window has significant influence in the dense scenario.

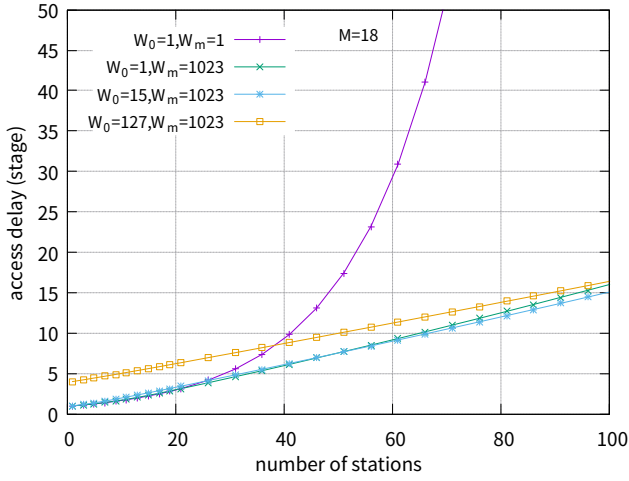
Different from DCF of legacy 802.11, the OFDMA-based MCRA mechanism is more flexible, with system parameters dynamically configured. A real-time algorithm is required to configure the system parameters dynamically. This paper takes the first step to catch some insight from the steady state behavior of the MCRA mechanism. In the future, transient analysis is necessary to generate a configuration algorithm.

## REFERENCES

- [1] "Cisco Visual Networking Index:Forecast and Methodology, 20152020," <http://www.cisco.com/c/en/us/solutions/collateral/service-provider/visual-networking-index-vni/complete-white-paper-c11-481360.pdf>, [Online; accessed on 13-June-2016].
- [2] E. Perahia and R. Stacey, *Next Generation Wireless LANS: 802.11 n and 802.11 ac*. Cambridge university press, 2013.
- [3] P. Zhou, H. Hu, H. Wang, and H.-h. Chen, "An efficient random access scheme for OFDMA systems with implicit message transmission," *IEEE transactions on wireless communications*, vol. 7, no. 7, pp. 2790–2797, 2008.
- [4] D. Shen and V. O. Li, "Performance analysis for a stabilized multi-channel slotted ALOHA algorithm," in *Personal, Indoor and Mobile Radio Communications, 2003. PIMRC 2003. 14th IEEE Proceedings on*, vol. 1. IEEE, 2003, pp. 249–253.



(a) System efficiency versus number of stations



(b) Access delay versus number of stations

Fig. 13: Example of Configuring  $OCW_{min}$ , given  $M = 18$ 

- [13] D.-J. Deng, S.-Y. Lien, J. Lee, and K.-C. Chen, "On Quality-of-Service Provisioning in IEEE 802.11 ax WLANs," *IEEE Access*.
- [14] T.-S. Ho and K.-C. Chen, "Performance analysis of IEEE 802.11 CSMA/CA medium access control protocol," in *proc. PIMRC*, vol. 96, 1996, pp. 407–411.
- [15] L. G. Roberts, "ALOHA packet system with and without slots and capture," *ACM SIGCOMM Computer Communication Review*, vol. 5, no. 2, pp. 28–42, 1975.

**Michael Shell** Biography text here.

PLACE  
PHOTO  
HERE

**John Doe** Biography text here.

**Jane Doe** Biography text here.

- [5] Y.-J. Choi, S. Park, and S. Bahk, "Multichannel random access in OFDMA wireless networks," *IEEE Journal on Selected Areas in Communications*, vol. 24, no. 3, pp. 603–613, 2006.
- [6] S. Kim, J. Cha, S. Jung, C. Yoon, and K. Lim, "Performance evaluation of random access for M2M communication on IEEE 802.16 network," in *Advanced Communication Technology (ICACT), 2012 14th International Conference on*. IEEE, 2012, pp. 278–283.
- [7] J.-B. Seo and V. C. Leung, "Design and analysis of backoff algorithms for random access channels in UMTS-LTE and IEEE 802.16 systems," *IEEE Transactions on Vehicular Technology*, vol. 60, no. 8, pp. 3975–3989, 2011.
- [8] A. B. Behroozi-Toosi and R. R. Rao, "Delay upper bounds for a finite user random-access system with bursty arrivals," *IEEE transactions on communications*, vol. 40, no. 3, pp. 591–596, 1992.
- [9] C.-H. Wei, G. Bianchi, and R.-G. Cheng, "Modeling and analysis of random access channels with bursty arrivals in OFDMA wireless networks," *IEEE Transactions on Wireless Communications*, vol. 14, no. 4, pp. 1940–1953, 2015.
- [10] H. Kwon, H. Seo, S. Kim, and B. G. Lee, "Generalized CSMA/CA for OFDMA systems: protocol design, throughput analysis, and implementation issues," *IEEE Transactions on Wireless Communications*, vol. 8, no. 8, pp. 4176–4187, August 2009.
- [11] *Draft 1.0, Part 11: Wireless LAN Medium Access Control (MAC) and Physical Layer (PHY) Specifications, Amendment 6: Enhancements for High Efficiency WLAN, 802.11ax*, pp. 1–376, Sep 2016.
- [12] G. Bianchi, "Performance analysis of the IEEE 802.11 distributed coordination function," *IEEE Journal on selected areas in communications*, vol. 18, no. 3, pp. 535–547, 2000.